
C-MCTS: Safe Planning with Monte Carlo Tree Search

Dinesh Parthasarathy, Georgios Kontes, Axel Plinge, Christopher Mutschler
Fraunhofer Institute for Integrated Circuits (IIS), Fraunhofer IIS
Nuremberg, Germany
{FirstName}. {LastName}@iis.fraunhofer.de

Abstract

Many real-world decision-making tasks, such as safety-critical scenarios, cannot be fully described in a single-objective setting using the Markov Decision Process (MDP) framework, as they include hard constraints. These can instead be modeled with additional cost functions within the Constrained Markov Decision Process (CMDP) framework. Even though CMDPs have been extensively studied in the Reinforcement Learning literature, little attention has been given to sampling-based planning algorithms such as MCTS for solving them. Previous approaches use Monte Carlo cost estimates to avoid constraint violations. However, these suffer from high variance which results in conservative performance with respect to costs. We propose Constrained MCTS (C-MCTS), an algorithm that estimates cost using a safety critic. The safety critic training is based on Temporal Difference learning in an offline phase prior to agent deployment. This critic limits the exploration of the search tree and removes unsafe trajectories within MCTS during deployment. C-MCTS satisfies cost constraints but operates closer to the constraint boundary, achieving higher rewards compared to previous work. As a nice byproduct, the planner is more efficient requiring fewer planning steps. Most importantly, we show that under model mismatch between the planner and the real world, our approach is less susceptible to cost violations than previous work.

1 Introduction

Monte Carlo Tree Search (MCTS) is a decision-making algorithm that employs Monte Carlo methods across the decision space, evaluates their outcome with respect to a given reward/objective, and constructs a search tree focusing on the most promising sequences of decisions [3, 22]. The success of MCTS can be attributed to the asymmetry of the trees constructed, which ensures better exploration of parts of the search space that are more promising. Also, the possibility of using neural networks as heuristics to guide the search tree has helped tackle complex and high-dimensional problems with large state and action spaces [20].

In spite of its successful application in several diverse domains, the standard, single-objective MCTS algorithm is unsuitable for a large class of real-world problems that apart from optimizing an objective function, also require a set of constraints to be fulfilled. These types of problems are usually modeled as Constrained Markov Decision Processes (CMDPs) [1] and specialized algorithms are used to solve the underlying constrained optimization problem.

Typical examples of such algorithms include approaches that rely on an expert knowledge base to create a safe action set [12, 18, 17], Lagrangian relaxation methods that update primal and dual variables incrementally online and learn safe policies [7, 19], approaches that learn separate reward and cost/constraint signals to train a safe-aware policy [2, 21, 25] and methods that utilize uncertainty-aware estimators like Gaussian Processes to balance the exploration/exploitation risk [23, 10]. Finally, a notable different way to model problems with constraints using temporal logic specifications [6], and incorporating them as soft constraints to solve a CMDP [8, 14].

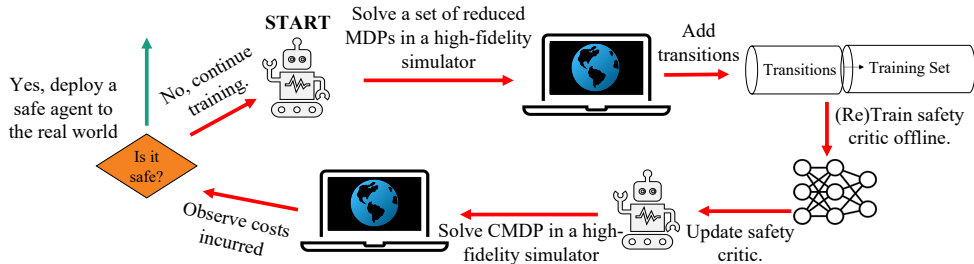


Figure 1: Simplified flow diagram illustrating the training phase in C-MCTS.

We propose a novel MCTS-based approach for solving Constrained Markov Decision Process (CMDP) problems called Constrained MCTS (C-MCTS),¹ see Fig. 1. We utilize a high-fidelity simulator to collect different sets of trajectories under different safety constraint satisfaction levels. Utilizing a simulator has several benefits, since violating cost-constraints has no real-world implications. Also, we can construct scenarios with high safety implications that have rare occurrences in the real world. The samples collected are used to train a safety critic offline, which is used during deployment within MCTS to make cost predictions and avoid tree expansion to unsafe states. The proposed method manages to construct a deeper search tree with fewer planning iterations compared to the state of the art, while discovering solutions that operate safely closer to the cost-constraint, thus leading to higher rewards.

The rest of the paper is structured as follows. Sec. 2 discusses relevant literature on MCTS for constrained and multi-objective sequential decision-making. Sec. 3 discusses background information and notation. Sec. 4 introduces C-MCTS. Sec. 5 shows experimental results. Sec. 6 concludes.

2 Related Work

Even though online planning and decision making under uncertainty for *continuous actions problems* is well-studied both in the Reinforcement Learning (RL) [5, 16, 13] and control [11] communities, MCTS to solve *discrete-action* CMDPs problems has only been little explored. To our knowledge, apart from the seminal work of Lee et al. [15], previous work extended the classical MCTS algorithm to multi-objective variants [9] that attempt to construct local [4] or global [24] Pareto fronts and determine the Pareto-optimal solution. These approaches report good results at the expense of higher computational costs, due to the need to compute a set of Pareto-optimal solutions.

In their seminal work, Lee et al. [15] proposed Cost-Constrained Monte Carlo Planning (CC-MCP), an MCTS algorithm to solve CMDPs. CC-MCP uses a Lagrange formulation and updates the Lagrange multiplier while constructing the search tree based on accumulated cost statistics. However, CC-MCP has two major shortcomings: (1) it requires a large number of planning iterations for the Lagrange multiplier to get well tuned (as it is tuned online and thus explores both unsafe and safe trajectories in the search tree), and (2) the performance is sub-optimal w.r.t costs, i.e., the agent acts conservatively. Moreover, the algorithm also relies on the planning model to calculate cost estimates, making it error-prone to use approximate planning models for fast planning at deployment.

Instead of tuning the Lagrange multiplier online C-MCTS varies this parameter in a pre-training phase to obtain different sets of trajectories with different safety levels. We obtain these samples from a high-fidelity simulator wherein violating cost-constraints is acceptable and use them to train a safety critic using Temporal Difference (TD) Learning, which has lower variance compared to Monte Carlo methods. The critic is an ensemble of neural networks that approximates the Q-function that predicts costs for state-action pairs. The learned safety critic is then used during deployment within MCTS to make cost predictions and to prune unsafe trajectories to avoid tree expansion to unsafe states. Since exploration is mostly limited to a safe search space, C-MCTS manages to construct a deeper search tree with fewer planning iterations compared to CC-MCP. We have systematically observed in our results that C-MCTS operates safely closer to the cost-constraint and collects higher rewards with fewer planning iterations as compared to CC-MCP. Additionally, as we learn cost estimates from a

¹<https://github.com/mutschcr/C-MCTS>

high-fidelity simulator in an offline phase, we are able to reduce the simulation-to-reality gap and operate safely even with approximate planning models as required for fast online planning.

3 Background

3.1 Constrained Markov Decision Processes (CMDPs)

CMDPs can be defined by the tuple $\langle S, A, \mathbb{T}, \mathbb{R}, \mathbb{C}, \hat{c}, \gamma, s_0 \rangle$ where S is the set of states s , A is the set of actions a , \mathbb{T} defines the probability of transitioning from $s \in S$ to $s' \in S$ for an action $a \in A$ executed at s , \mathbb{R} is a reward function that returns a one-step reward for a given action a at a state s , \mathbb{C} is the set of M cost functions, \hat{c} is a set of constraints for these costs functions, $\gamma \in [0, 1)$ is the discount factor, and $s_0 \in S$ is the initial start state. The optimal policy π^* in such a framework is

$$\begin{aligned} \max_{\pi} V_{\mathbb{R}}^{\pi}(s_0) &= \mathbb{E}_{\pi} \left[\sum_{t=0}^T \gamma^t \mathbb{R}(s_t, a_t) | s_0 \right] \\ \text{s.t. } V_{\mathbb{C}_m}^{\pi}(s_0) &= \mathbb{E}_{\pi} \left[\sum_{t=0}^T \gamma^t \mathbb{C}_m(s_t, a_t) | s_0 \right] \leq \hat{c}_m \quad \forall m \in \{1, 2, 3, \dots, M\}, \end{aligned} \quad (1)$$

where $V_{\mathbb{R}}$ is the expected discounted cumulative reward, and $V_{\mathbb{C}_m}$ is the expected discounted cumulative cost for each of the M cost functions.

3.2 Cost-Constrained Monte Carlo Planning (CC-MCP)

MCTS is a decision-making algorithm that can search large combinatorial spaces represented by trees. The search tree consists of nodes representing each state uniquely, and edges representing actions that connect these nodes. The algorithm is used iteratively to explore the state space and build statistical evidence about different decision paths. Based on the gathered statistics, an optimal set of actions is taken such that the expected cumulative reward is maximized. Each iteration of MCTS consists of four phases: (i) selection, (ii) expansion, (iii) simulation, and (iv) backpropagation.

CC-MCP is an MCTS-based algorithm for solving CMDPs wherein the CMDP problem is formulated as an Linear Program (LP), and then the dual formulation is solved as follows:

$$\begin{aligned} \min_{\lambda \geq 0} & [\nu_{\lambda}^* + \lambda^T \hat{c}] \\ \nu_{\lambda} &= V_{\mathbb{R}} - \lambda^T V_{\mathbb{C}} \end{aligned} \quad (2)$$

Here, ν_{λ}^* is the optimal value function for a scalarized reward function $\mathbb{R} - \lambda^T \mathbb{C}$. $V_{\mathbb{R}}, V_{\mathbb{C}}$ are the expected discounted cumulative reward and costs respectively, and \hat{c} are the cost constraints. As the objective function in Eq. 2 is piecewise-linear and convex over λ [15], λ can be updated using the gradient information $V_{\mathbb{C}}^* - \hat{c}$, where $V_{\mathbb{C}}^*$ are the costs incurred for an optimal policy with a fixed λ . Hence, CMDP can be solved by iterating the following three steps: (i) Solve MDP with a scalarized reward $\mathbb{R} - \lambda^T \mathbb{C}$, (ii) Evaluate $V_{\mathbb{C}}^*$ for this policy, (iii) Update λ using the gradient information. Steps (i) and (ii) can also be interleaved at a finer granularity, and this is the idea behind CC-MCP, where λ is updated at every MCTS iteration based on the Monte Carlo cost estimate $\hat{V}_{\mathbb{C}}$ at the root node of the search tree.

4 Method

We formulate C-MCTS as a variant of MCTS to solve CMDPs. First, we generate offline data from simulations to explore the state and action space exhaustively. We use these data to train an ensemble of neural networks to approximate the state-action value function $\hat{Q}_c(s, a)$, i.e., the discounted cumulative cost for an action at a given state. The trained networks (also referred to as safety critics) are then used within MCTS. The agreement of the networks in the ensemble identifies state-action pairs that have not been visited in the offline phase and the corresponding predictions are ignored. For other inputs (that are in-distribution) the Q-value predictions are used to identify action sequences that are likely to violate the cost constraint to limit tree expansion to a safe search space. To this end, C-MCTS consists of a (pre-)training phase (Sec. 4.1) and a deployment phase (Sec. 4.2).

4.1 Training Phase

As described previously, before deploying the planner to the real world, we train our safety critic by collecting samples from a high-fidelity simulator. In the simulated environment, we use MCTS to solve the same CMDP by modeling the safety boundary using soft constraints within the Markov Decision Process (MDP) framework. Soft constraints are imposed by augmenting the reward function with an additional term $-\lambda^T C$. Varying the value of the Lagrange multiplier λ produces a set of MDPs with different safety levels. This encourages exploration and helps in creating a rich offline data set for training the safety critic. Generating offline data and training the safety critic are steps within the training phase interleaved one after the other. After each training loop, the trained safety critic is used within MCTS to solve the original constrained problem in simulation. The training loop is terminated only if the problem is solved safely in simulation. Otherwise, we continue the training loop and gather more training samples.

While creating a set of reduced MDPs to generate our training set we use a scheduling strategy for λ that encourages exploration closer to the safety boundary, see Fig. 2. Each MDP is solved repeatedly generating multiple episodes. Each member of the MDP set is added in succession based on the agent’s performance on the last/previous MDP. First, we initialize λ with zero and create the first MDP (which likely results in an over-risky behavior). The average discounted costs over all episodes (\bar{V}_C) are evaluated and compared to the cost constraint (\hat{c}). λ is updated based on the difference between these values, $\bar{V}_C - \hat{c} = \Delta c$, and this sets up the next MDP. This is repeated until λ converges to a value λ^* that solves the CMDP optimally, i.e., where the incurred costs are just below the cost-constraint. We use an additional parameter ϵ for this termination criteria: $\hat{c} - \epsilon \leq \bar{V}_C \leq \hat{c}$. $\frac{\alpha_0}{n}$ is the step size which decreases with every loop iterate n . α_0 is a fixed constant. Hence, more training samples are generated close to the safety boundary, helping the safety critic to learn the safety boundary more accurately.

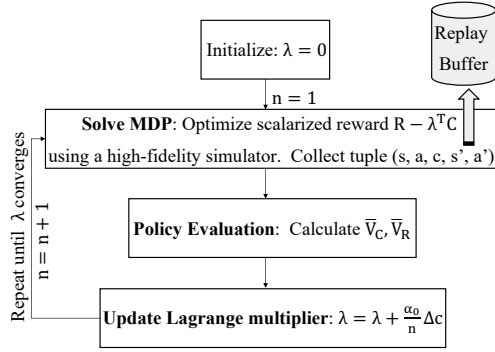


Figure 2: Create a set of reduced MDPs during the training phase of C-MCTS.

Algorithm 1: C-MCTS | Using a learned safety critic in MCTS.

```

1 repeat
2    $\mathcal{N}_{cur} \leftarrow \mathcal{N}_{root}$  // get root node
   // SELECTION
3   while  $\mathcal{N}_{cur}$  is not terminal do
4      $\mathcal{N}_{cur} \leftarrow \text{SELECT}(\mathcal{N}_{cur})$  // traverse search tree using UCT algorithm
5      $\mathcal{P} \leftarrow \mathcal{P} + [\mathcal{N}_{cur}]$  // store traversal path
6   end
7    $\mathcal{N}_{leaf} \leftarrow \mathcal{N}_{cur}$  // store selected leaf node
   // EXPANSION
8   i. Get safety critic outputs  $(\hat{\mu}, \hat{\sigma})$  for all actions  $a \in A$  from  $\mathcal{N}_{leaf}$ .
9   ii. Consider predictions with standard deviation output  $(\hat{\sigma})$  less than the ensemble
       threshold  $(\sigma_{max})$  i.e. let  $A_{feasible} = \{a : \hat{\sigma}_a \leq \sigma_{max}\}$ .
10  iii. Calculate the cost estimate  $V_C$  for actions  $a \in A_{feasible}$ .
11  iv. Find cost-violating actions i.e. let  $A_{unsafe} = \{a \in A_{feasible} : V_C(a) > \hat{c}\}$ .
12  v. Expand tree for branches without unsafe actions,  $a \in A \setminus A_{unsafe}$ .
   // SIMULATION
13   $\hat{V}_R \leftarrow \text{ROLLOUT}(\mathcal{N}_{leaf})$  // get monte carlo reward estimate
   // BACKPROPAGATION
14   $\text{BACKUP}(\hat{V}_R, \mathcal{P})$  // update tree statistics along traversed path
15 until maximum planning iterations is reached

```

We use the collected offline data to train an ensemble of neural networks with different weight initializations to predict the Q-values for the incurred costs. The trainable parameters of this network are optimized to minimize the mean-squared Bellmann error which uses a low variance one-step TD-target. The aggregated ensemble output $(\hat{\mu}, \hat{\sigma})$ provides a mean and a standard deviation computed from the individual member’s outputs, which we then use within MCTS. As MCTS explores the state space exhaustively in simulation, some state-action pairs are likely *out-of-distribution* from the training set. Hence, the safety critic output with an ensemble standard deviation greater than a set threshold $\hat{\sigma} > \sigma_{max}$ can be used to identify and ignore those samples and predictions.

4.2 Deployment Phase

The trained safety critic is used during the expansion phase in MCTS, see Alg. 1. Other phases (selection, simulation, backpropagation) are identical to the vanilla MCTS algorithm. At the expansion phase, we try to expand the search tree from the leaf node along different branches corresponding to different actions. First, based on the safety critic’s output we filter out predictions that we cannot trust (corresponding to high ensemble variance) and create a reduced action set (lines 8-9). The safety of each action from this set is evaluated based on the safety critic’s output predicting expected cumulative costs from the leaf. This is summed up with the one-step costs stored in the tree from the root node to the leaf node. If this total cost estimate (V_C) is greater than the cost constraints (\hat{c}), then we prune the corresponding branches, while other branches are expanded (lines 10-12). These steps, when repeated over multiple planning iterations create a search tree exploring a safe search space.

5 Evaluation

We evaluate our method by comparing its performance with our baseline CC-MCP [15] on *Rocksam-ple* and *Safe Gridworld* environments (see Sec. 5.1): we study the planning efficiency (Sec. 5.2.1) and safety under sim2real gaps (Sec. 5.2.2). As another baseline, assuming an oracle that gives us an optimal Lagrange multiplier λ^* , we measure the performance of a single objective vanilla MCTS algorithm maximizing $R - \lambda^{*T}C$ on *Rocksam-ple* environments. Further, we analyze the sensitivity of C-MCTS to parameters affecting its safety. We study the safety of the agent at deployment for different (i) lengths of planning iterations during training (Sec. 5.3.1) (ii) values of ensemble threshold during deployment (Sec. 5.3.2), and (iii) training simulators with different accuracies (Sec. 5.3.3).

5.1 Environments

***Rocksam-ple* (n,m)** is an $n \times n$ -sized grid with m randomly placed rocks, some of them being good and others being bad. The goal is to collect as many good rocks as possible and exit the grid. The positions of the rocks are known in advance, but the quality of the rocks is unknown. The agent can either move through the grid or make noisy measurements to sense the quality, which is correct with a probability of $(2^{-d/d_0} + 1)/2$, where d is the Euclidean distance of the agent from the corresponding rock and d_0 is a constant, i.e., being less accurate at a larger distance. The agent receives a positive reward for exiting the grid and for collecting good rocks, a negative reward for collecting bad rocks, exiting at the wrong end, and for sampling empty grid locations. The agent incurs a +1 cost when measuring the quality of a single rock. The discounted cost over an episode cannot exceed 1, and this is the cost-constraint. The discount factor γ is set to 0.95. To maximize rewards (collecting good rocks) with constraints (number of sensor measurements) the agent may only use a limited number of measurements at a reasonable proximity to the rocks. More details can be found in the appendix (Sec. A.1.1).

Safe Gridworld is a 8×8 grid with the goal to find the shortest path from a start (bottom left) to a goal (top right) position while avoiding unsafe regions. There are stochastic transition dynamics in eight squares at the top of the grid (winds blowing push the agent down by some probability). We will vary this probability to account for simulator mismatch in the experiment in Sec. 5.2.2). The agent receives a reward of -1 per time step, a reward of +100 on reaching the goal state, and a -1000 penalty for exiting the grid. Visiting unsafe areas incurs a cost of +1. The agent should only traverse safe squares, effectively implying a discounted cost over an episode of 0. That’s why we impose a cost-constraint of 0. The discount factor γ is set to 0.95. More details can be found in the appendix (Sec. A.1.2).

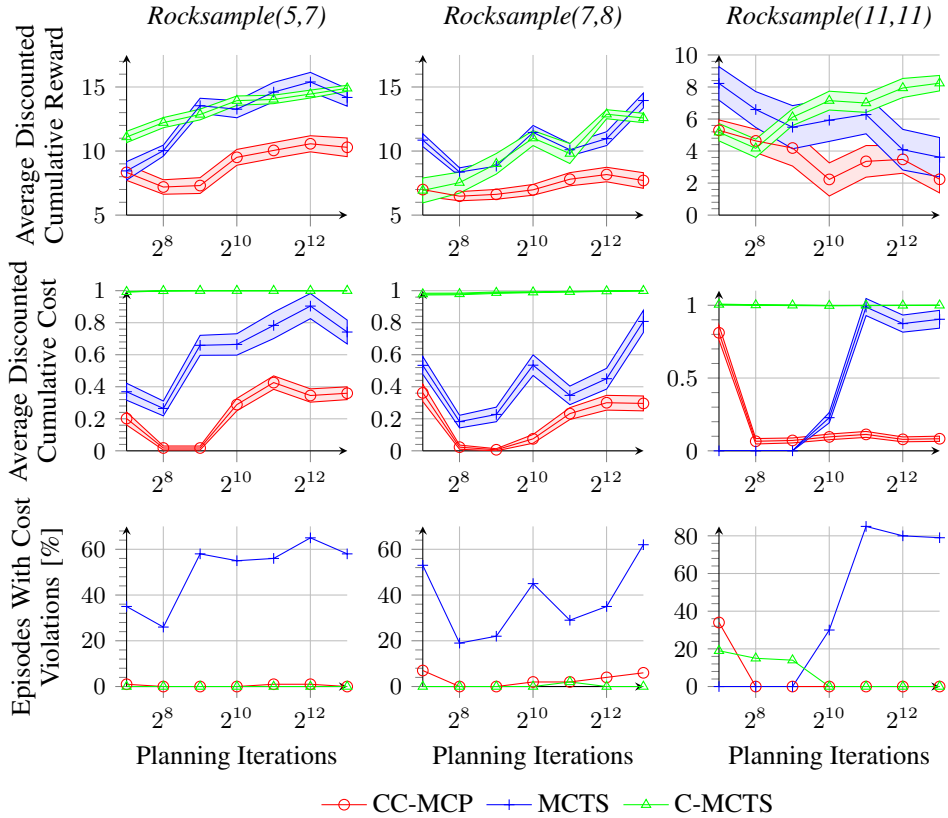


Figure 3: Comparing performance of C-MCTS, MCTS and CC-MCP on different configurations of *Rocksampler* environments evaluated on 100 episodes.

5.2 Results

We measure the performance of the agent on different sizes and complexities of *Rocksampler* environments, with C-MCTS, CC-MCP, and a vanilla MCTS with a fixed λ set to 0.7 for *Rocksampler(5, 7)*, *Rocksampler(7, 8)*, and 5.0 for *Rocksampler(11, 11)*. The values were hand-tuned to balance reward and cost, with lower λ increasing cost violations and higher λ reducing rewards. We compare the reward, cost and number of cost violations of these planning methods across different planning iterations.

C-MCTS obtains higher rewards compared to the state-of-the-art CC-MCP while still operating within the cost-constraint (see Fig. 3, top row). The reward for C-MCTS increases with the number of planning iterations. Also, the agent operates consistently below the cost-constraint (see Fig. 3, middle row), very close to the safety boundary while CC-MCP acts conservatively w.r.t costs, hence performing sub-optimally w.r.t rewards. The costs incurred have a high variance across different episodes. In *Rocksampler(7,8)* the variance is 1.35×10^{-1} (averaged across the planning spectrum). For C-MCTS the variance is only 1.31×10^{-3} , as we use TD learning instead of Monte Carlo methods to learn cost estimates. Hence, the total number of cost violations is lower for C-MCTS compared to the other methods, in spite of operating closest to the safety constraint (see Fig. 3, bottom row).

Vanilla MCTS with the penalty term obtains much higher rewards compared to CC-MCP. This is because we fix λ to a near-optimal value for each environment and avoid tuning it online. This ensures faster convergence to optimality. MCTS operates closer to the cost-constraint when compared to CC-MCP but still has a high variance. The total number of cost violations is very high. C-MCTS, when compared to vanilla MCTS, is safer and obtains equally high rewards or in some cases even acts better (e.g., *Rocksampler(11, 11)*).

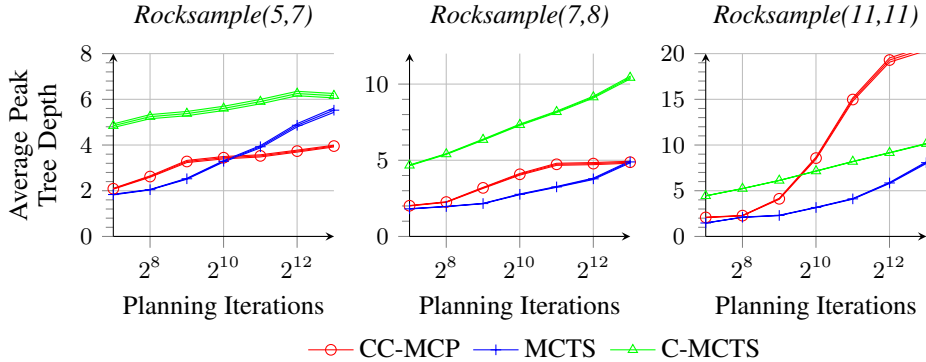


Figure 4: Maximum depth of the search tree for C-MCTS, MCTS and CC-MCP on different rock-sample configurations averaged over 100 episodes.

5.2.1 Planning efficiency

We compare the planning efficiency of the three methods for the same set of experiments addressed previously. The comparison is done based on the depth of the search tree, given a specific computational budget (i.e., a fixed number of planning iterations). This comparison is qualitative and is used to evaluate the effectiveness of different planning algorithms.

Fig. 4 shows that C-MCTS performs a more narrow search for the same number of planning iterations. The peak tree depth when averaged over 100 episodes is the highest for C-MCTS. In C-MCTS the exploration space is restricted using the safety critic, and this helps in efficient planning. In Rocksampler(11, 11) the peak tree depth of CC-MCP is high in spite of having a sub-optimal performance. This is probably because the Lagrange multiplier in CC-MCP gets stuck in a local maximum and is unable to find a global solution.

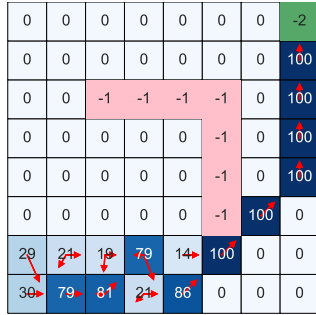
5.2.2 Reducing the simulation-to-reality gap

Online planners often resort to approximate models of the real world for fast planning and to account for real-time decision requirements. Those model imperfections can lead to safety violations while a high-fidelity model during deployment is infeasible due to computational constraints. We resolve this dilemma by learning safety constraints before deployment from a simulator that has a higher fidelity compared to the planning model. The benefit of such an approach is shown using a synthetically constructed *Safe Gridworld* scenario (see Sec. A.1.2).

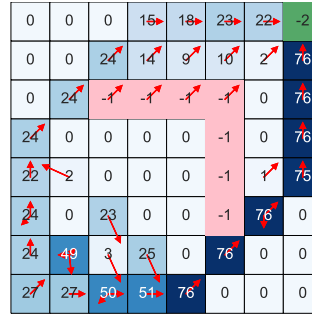
In this setup, we use a planning simulator that models the environment dynamics approximately, and a training simulator (for the safety critic) that captures the dynamics more accurately. In the planning simulator, all the transition dynamics are accurately modeled, except the blue squares with winds (Fig. 7 right). The transitions here are determined by the action selection, and the stochasticity due to wind effects is not considered. The training simulator models the transitions in these regions more accurately, but with some errors. The agent in the blue squares moves down with a probability of 0.25, as compared to the real-world configuration where we model the probability of this transition with 0.3. The behavior of the agent with C-MCTS and CC-MCP is observed on these defined configurations. C-MCTS was trained and evaluated for 2^9 planning iterations, while CC-MCP was evaluated for 2^{20} planning iterations. The latter was set to a higher planning budget to obtain the most optimal behavior.

Fig. 5 shows the number of state visitations of C-MCTS (left) and CC-MCP (right). The agent using CC-MCP takes both of the possible paths (going to the top and going to the right), avoiding the unsafe region (in pink) to reach the goal state. This would be optimal in the absence of the windy squares, but here it leads to cost violations due to inaccurate cost estimates². C-MCTS on the other hand avoids the path from the top and only traverses through the two right-most columns to avoid the unsafe region. The safety critic being trained on more realistic samples from the higher-fidelity

²Of course also the variance could play a minor role but we designed the setup to focus on the dynamics mismatch between the planner and the actual environment, which is much more prevalent here.



(a) C-MCTS with 0% cost violations.



(b) CC-MCP with 11% cost violations.

Figure 5: State visitations aggregated over 100 episodes. The length of the arrows is proportional to the number of action selections. Values of -1 and -2 denote unsafe cells and the goal cell, respectively.

training simulator identifies the path from the top as unsafe. This leads to zero cost violations leading to optimal safe behavior.

5.3 Exploring training and deployment strategies for safe behavior

We vary hyper-parameters in the training and deployment of a safety critic and identify key parameters that impact the safety of the agent. The experiments were conducted on a `Rocksampl(7, 8)` environment, and the results were averaged over 100 runs. We observed that the performance of C-MCTS is sensitive to the length of the planning horizon during training (Sec. 5.3.1), to the threshold used for the ensemble during deployment (i.e., σ , see Sec. 5.3.2), and the accuracy of the training simulator (i.e., via varying d_0 , see Sec. 5.3.3). To study the effect of these parameters we optimized the other algorithmic parameters, i.e., α_0 (initial step size to update λ) and ϵ (termination criterion for training loop), with a grid search. For each of the experiments we then selected a reasonably performing configuration (i.e., Sec. 5.3.1: $\alpha_0=4$, $\epsilon=0.1$; Sec. 5.3.2: $\alpha_0=8$, $\epsilon=0.3$; Sec. 5.3.3: $\alpha_0=1$, $\epsilon=0.1$) and ablated the respective hyperparameters, i.e., planning horizon in training, σ , and d_0 .

5.3.1 Length of planning horizon during training

We conduct experiments with different sets of hyper-parameters to study the effect of using different planning iterations during the safety critic training, and evaluate the performance of the agent during deployment.

From Fig. 6 (left column) we can observe that the safety critic trained with a longer planning horizon operates closer to the safety boundary. This is because the trained safety critic learns to predict costs for a near-optimal policy and hence discerns the safety boundary more accurately. On the other hand, the safety critic trained with a smaller planning horizon learns cost estimates from a sub-optimal policy leading to cost violations during deployment.

5.3.2 Ensemble threshold during deployment

We study the effect of using different standard deviation thresholds in the neural network ensemble during deployment. We observe the safety of the agent during deployment for ensemble threshold values $\sigma_{max} = 0.1$ and $\sigma_{max} = 0.5$.

Fig. 6 (middle column) shows that the cost incurred exceeds the cost-constraint if $\sigma_{max} = 0.1$, but the agent performs safely within the cost-constraint with a far lesser number of cost violations if $\sigma_{max} = 0.5$. We prune unsafe branches during planning only when the predictions between the individual members of the ensemble align with each other. Setting $\sigma_{max} = 0.1$ is a tight bound resulting in most of the predictions of the safety critic being ignored. Using a higher threshold with $\sigma_{max} = 0.5$ ensures that only large mismatches between the predictions of the individual members (corresponding to out-of-distribution inputs) are ignored, and the rest are used during planning. This results in the agent performing safely within the cost-constraint, but yet not too conservatively.

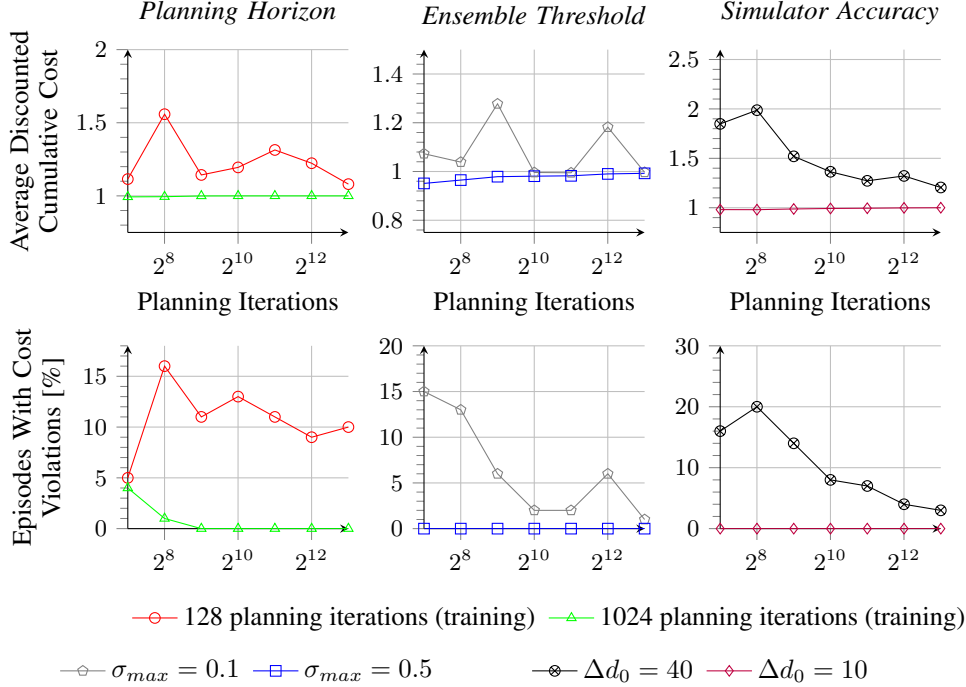


Figure 6: Comparing safety for different training/deployment strategies, i.e., using different planning horizons during training (left), deploying with different ensemble thresholds (middle), and collecting training samples from simulators of different accuracies (right).

5.3.3 Accuracy of the training simulator

We study the performance of C-MCTS when trained on imperfect simulators. On the Rocksample environment, the sensor characteristics measuring the quality of the rock are defined by the constant d_0 (see Sec. A.1.1). In the following experiments, we overestimate the sensor accuracy in our training simulator by choosing d_0^{sim} with error Δd_0 and observe the safety of the agent in the real world when trained on simulators with different values of Δd_0 .

Fig. 6 (right column) shows the results. The values of Δd_0 set to 10 and 40 corresponds to a maximum prediction error of 11.7% and 32.5%, respectively. When $\Delta d_0 = 40$ the agent operates at a greater distance from the cost-constraint. The reason for cost violations is that the safety critic has been trained to place too much trust in the sensor measurements due to the simulation-to-reality gap. With a smaller gap ($\Delta d_0 = 10$) the agent performs safer.

6 Conclusion

We presented an MCTS-based approach to solving CMDPs that learns the cost-estimates in a pre-training phase from simulated data and that prunes unsafe branches of the search tree during deployment. In contrast to previous work, C-MCTS does not need to tune a Lagrange multiplier online, which leads to better planning efficiency and higher rewards. In our experiments on Rocksample environments, C-MCTS achieved maximum rewards surpassing previous work by 41%, 57%, and 55% for small, medium, and large-sized grids respectively, while maintaining safer performance. As cost is estimated from a lower variance TD target the agent can operate close to the safety boundary with minimal constraint violations. C-MCTS is also suited for problems using approximate planning models for fast inference, but having to adhere to stringent safety norms. In our Safe Gridworld setup, we demonstrate that even with an approximate planning model, the notion of safety can be learned separately using a more realistic simulator, resulting in zero constraint violations and improved safety behavior.

References

- [1] E. Altman. *Constrained Markov Decision Processes*. Chapman and Hall, 1999.
- [2] H. Bharadhwaj, A. Kumar, N. Rhinehart, S. Levine, F. Shkurti, and A. Garg. Conservative safety critics for exploration. *arXiv preprint arXiv:2010.14497*, 2020.
- [3] C. Browne, E. Powley, D. Whitehouse, S. Lucas, P. Cowling, P. Rohlfshagen, S. Tavener, D. Perez Liebana, S. Samothrakis, and S. Colton. A survey of monte carlo tree search methods. *IEEE Transactions on Computational Intelligence and AI in Games*, 4:1:1–43, 03 2012.
- [4] W. Chen and L. Liu. Pareto monte carlo tree search for multi-objective informative planning. In *Proceedings of Robotics: Science and Systems*, Freiburg/Breisgau, Germany, June 2019.
- [5] K. Chua, R. Calandra, R. McAllister, and S. Levine. Deep reinforcement learning in a handful of trials using probabilistic dynamics models. *Advances in neural information processing systems*, 31, 2018.
- [6] S. Demri and P. Gastin. Specification and verification using temporal logics. In *Modern Applications of Automata Theory*, pages 457–493. Co-Published with Indian Institute of Science (IISc), Bangalore, India, July 2012.
- [7] D. Ding, K. Zhang, T. Basar, and M. R. Jovanovic. Natural policy gradient primal-dual method for constrained markov decision processes. In *Proceedings of the 34th International Conference on Neural Information Processing Systems, NIPS’20*, Red Hook, NY, USA, 2020. Curran Associates Inc.
- [8] M. Guo and M. M. Zavlanos. Probabilistic motion planning under temporal tasks and soft constraints. *IEEE Transactions on Automatic Control*, 63(12):4051–4066, 2018.
- [9] C. F. Hayes, M. Reymond, D. M. Roijers, E. Howley, and P. Mannion. Monte carlo tree search algorithms for risk-aware and multi-objective reinforcement learning. *Autonomous Agents and Multi-Agent Systems*, 37(2), Apr. 2023.
- [10] L. Hewing, J. Kabzan, and M. N. Zeilinger. Cautious model predictive control using gaussian process regression. *IEEE Transactions on Control Systems Technology*, 28(6):2736–2743, 2019.
- [11] L. Hewing, K. P. Wabersich, M. Menner, and M. N. Zeilinger. Learning-based model predictive control: Toward safe learning in control. *Annual Review of Control, Robotics, and Autonomous Systems*, 3:269–296, 2020.
- [12] C.-J. Hoel, K. Driggs-Campbell, K. Wolff, L. Laine, and M. J. Kochenderfer. Combining planning and deep reinforcement learning in tactical decision making for autonomous driving. *IEEE Transactions on Intelligent Vehicles*, 5(2):294–305, 2020.
- [13] A. K. Jayant and S. Bhatnagar. Model-based safe deep reinforcement learning via a constrained proximal policy optimization algorithm. In S. Koyejo, S. Mohamed, A. Agarwal, D. Belgrave, K. Cho, and A. Oh, editors, *Advances in Neural Information Processing Systems*, volume 35, pages 24432–24445. Curran Associates, Inc., 2022.
- [14] K. C. Kalagarla, K. Dhruva, D. Shen, R. Jain, A. Nayyar, and P. Nuzzo. Optimal control of partially observable markov decision processes with finite linear temporal logic constraints. In J. Cussens and K. Zhang, editors, *Proceedings of the Thirty-Eighth Conference on Uncertainty in Artificial Intelligence*, volume 180 of *Proceedings of Machine Learning Research*, pages 949–958. PMLR, 01–05 Aug 2022.
- [15] J. Lee, G.-H. Kim, P. Poupart, and K.-E. Kim. Monte-carlo tree search for constrained pomdps. In *Proceedings of the 32nd International Conference on Neural Information Processing Systems, NIPS’18*, page 7934–7943, Red Hook, NY, USA, 2018. Curran Associates Inc.
- [16] Z. Liu, H. Zhou, B. Chen, S. Zhong, M. Hebert, and D. Zhao. Constrained model-based reinforcement learning with robust cross-entropy method, 2021.
- [17] B. Mirchevska, C. Pek, M. Werling, M. Althoff, and J. Boedecker. High-level decision making for safe and reasonable autonomous lane changing using reinforcement learning. In *2018 21st International Conference on Intelligent Transportation Systems (ITSC)*, pages 2156–2162. IEEE, 2018.
- [18] A. Mohammadhasani, H. Mehrivash, A. Lynch, and Z. Shu. Reinforcement learning based safe decision making for highway autonomous driving. *arXiv preprint arXiv:2105.06517*, 2021.
- [19] S. Paternain, M. Calvo-Fullana, L. F. O. Chamon, and A. Ribeiro. Learning safe policies via primal-dual methods. In *2019 IEEE 58th Conference on Decision and Control (CDC)*, page 6491–6497. IEEE Press, 2019.
- [20] J. Schrittwieser, I. Antonoglou, T. Hubert, K. Simonyan, L. Sifre, S. Schmitt, A. Guez, E. Lockhart, D. Hassabis, T. Graepel, T. Lillicrap, and D. Silver. Mastering atari, go, chess and shogi by planning with a learned model. *Nature*, 588:604–609, 12 2020.
- [21] K. Srinivasan, B. Eysenbach, S. Ha, J. Tan, and C. Finn. Learning to be safe: Deep rl with a safety critic. *arXiv preprint arXiv:2010.14603*, 2020.

- [22] M. Świechowski, K. Godlewski, B. Sawicki, and J. Mańdziuk. Monte carlo tree search: a review of recent modifications and applications. *Artificial Intelligence Review*, July 2022.
- [23] A. Wachi, Y. Sui, Y. Yue, and M. Ono. Safe exploration and optimization of constrained MDPs using gaussian processes. *Proceedings of the AAAI Conference on Artificial Intelligence*, 32(1), Apr. 2018.
- [24] W. Wang and M. Sebag. Multi-objective Monte-Carlo tree search. In S. C. H. Hoi and W. Buntine, editors, *Proceedings of the Asian Conference on Machine Learning*, volume 25 of *Proceedings of Machine Learning Research*, pages 507–522, Singapore Management University, Singapore, 04–06 Nov 2012. PMLR.
- [25] Q. Yang, T. D. Simão, S. H. Tindemans, and M. T. J. Spaan. Safety-constrained reinforcement learning with a distributional safety critic. *Machine Learning*, 112(3):859–887, June 2022.

A Supplementary Material

A.1 Environments

A.1.1 Rocksample

The environment is defined as a grid with $n \times n$ squares with m rocks randomly placed, some being good and others bad (see Fig. 7, left). A specific Rocksample setup is defined by the nomenclature $\text{Rocksample}(n, m)$. A rover (agent) starting from the left is tasked to collect as many good rocks as possible and exit the grid to the right. The positions of the rocks are known in advance, but the quality of the rocks is unknown. The agent can move up, down, right, and left, sample a rock or make measurements to sense the quality of a rock. The total number of possible actions is hence $5 + m$. The agent is equipped with a noisy sensor to measure the quality of a rock with a probability of accuracy $(2^{-d/d_0} + 1)/2$, where d is the Euclidean distance of the agent from the corresponding rock and d_0 is a constant. The number of measurements that the agent can perform is constrained. Trying to maximize rewards (collecting good rocks) with constraints (number of sensor measurements) encourages the agent to use a limited number of measurements at a reasonable proximity to the rocks, wherein the sensor readings can be trusted. At each time step the agent observes its own position and the positions of the rocks with the updated probabilities.

We formulate the task within the CMDP framework by additionally defining a reward structure, cost function, and a cost-constraint. The agent is rewarded a +10 reward for exiting the grid from the right or for collecting a good rock. A -10 penalty is received for each bad rock collected, and a -100 penalty is given when the agent exits the grid to the other sides or if the agent tries to sample a rock from an empty grid location. The agent incurs a +1 cost when measuring the quality of a single rock. The discounted cost over an episode cannot exceed 1, and this is the cost-constraint. The discount factor γ is set to 0.95.

A.1.2 Safe Gridworld

We additionally propose a new problem: *Safe Gridworld*. The environment is defined as 8×8 grid where an agent from the bottom left region is tasked to find the shortest path to reach the top right square avoiding unsafe squares on the way (see Fig. 7, right). The agent can move to the neighboring squares and has a total of 9 action choices. The transition dynamics in all squares are deterministic except the 8 squares at the top which are stochastic. These squares have winds blowing from the top to the bottom forcefully pushing the agent down by one square with a probability of 0.2, independent of the action chosen by the agent (we will vary this probability to account for simulator mismatch in the experiment in Sec. 5.2.2). Otherwise, the transition is guided by the agent’s action.

The agent receives a reward of +100 on reaching the goal state, a -1000 penalty for exiting the grid, and a -1 penalty otherwise until the terminal state is reached. Entering an unsafe square incurs a cost of +1. The agent should only traverse safe squares, and the discounted cost over an episode is 0. The cost-constraint imposes this as a constraint and is set to 0. The discount factor γ is set to 0.95.

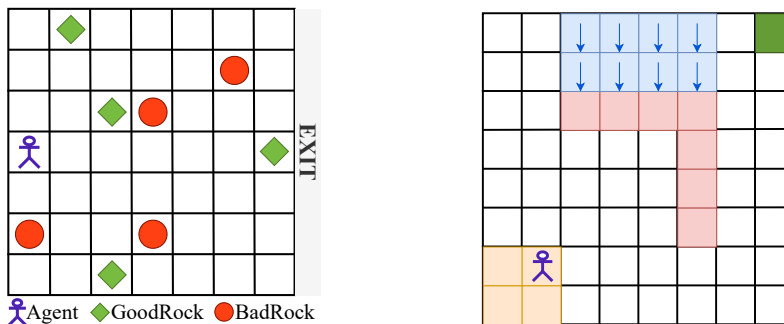


Figure 7: Environments: (left) exemplary $\text{Rocksample}(7, 8)$ environment, i.e., a 7×7 rocksample environment with 8 rocks randomly placed; (right) exemplary Safe Gridworld environment, where the colors denote start cells (yellow), the goal cell (green), unsafe cells (pink), and windy cells (blue).

A.2 Training Details & Compute

The training and evaluation were conducted on a single Intel Xeon E3-1240 v6 CPU. The CPU specifications are listed below.

Table 1: Specifications of Intel Xeon E3-1240 v6

Component	Specification
Generation	Kaby Lake
Number of Cores	4
Hyper-Threading (HT)	Disabled
Base Frequency	3.70 GHz
RAM	32 GB
SSD	960 GB

No GPU accelerators were used as the C-MCTS implementation was not optimized for efficient GPU resource utilization. The hyperparameters chosen for training the safety critic in the primary results (Fig. 3) are summarized in Table 2.

Table 2: Key hyperparameters to train the safety critic.

Environment	α_0	ϵ	σ_{max}	Planning Iterations
Rocksample(5, 7)	8	0.1	0.5	1024
Rocksample(7, 8)	4	0.1	0.5	1024
Rocksample(11, 11)	12	0.1	0.5	512
Safe Gridworld	10	0.1	0.2	512

A.3 Broader Impact

While C-MCTS mitigates the reliance on the planning model to meet cost constraints through pre-training in a high-fidelity simulator, there may still be sim-to-reality gaps when learning cost estimates. This introduces the possibility of encountering unforeseen consequences in real-world scenarios. In the context of using C-MCTS in a human-AI interaction task, if minority groups are not adequately represented in the training simulator, inaccurate cost estimates might lead to potential harm to humans. However, C-MCTS addresses these gaps more effectively than previous methods by leveraging a more relaxed computational budget during the training phase (fast inference is only required during deployment). This allows more accurate modeling of the real world to include rare edge scenarios.